

# Effects of the field modulation on the Hofstadter's spectrum

Gi-Yeong Oh\*

*Department of Basic Science, Ansung National University,  
Kyonggi-do 456-749, Korea  
(June 16, 2021)*

We study the effect of spatially modulated magnetic fields on the energy spectrum of a two-dimensional (2D) Bloch electron. Taking into account four kinds of modulated fields and using the method of direct diagonalization of the Hamiltonian matrix, we calculate energy spectra with varying system parameters (i.e., the kind of the modulation, the relative strength of the modulated field to the uniform background field, and the period of the modulation) to elucidate that the energy band structure sensitively depends on such parameters: Inclusion of spatially modulated fields into a uniform field leads occurrence of gap opening, gap closing, band crossing, and band broadening, resulting distinctive energy band structure from the Hofstadter's spectrum. We also discuss the effect of the field modulation on the symmetries appeared in the Hofstadter's spectrum in detail.

PACS numbers: 71.28.+d, 71.25.-s, 73.20.Dx, 71.45.Gm

## I. INTRODUCTION

The problem of a 2D Bloch electron under a uniform magnetic field has been intensively studied for several decades,<sup>1</sup> and it is well known that the energy spectrum is characterized by the Hofstadter's butterfly showing a fractal nature.<sup>2</sup> Recently the problem has attracted theoretically renewed interest in connection with various phenomena such as the quantum Hall effect,<sup>3</sup> the flux state model for high- $T_c$  superconductivity,<sup>4</sup> and the mean-field transition temperature of superconducting networks or Josephson junction arrays.<sup>5</sup> Besides, recent advance in submicron technology that makes it possible to fabricate any desired microstructures has stimulated experimental study to find indication of the Hofstadter's spectrum and its effect on the transport and optical properties.<sup>6-9</sup> In parallel with this problem, the study on 2D electron systems under nonuniform (either disordered<sup>10</sup> or periodic<sup>11-26</sup>) magnetic fields has been extensively performed, and lots of interesting characteristics in the energy spectral and transport properties have been elucidated.

Though the problem of a 2D Bloch electron under spatially modulated magnetic fields has attracted less attention compared with the problem of 2D electron gas under spatially modulated magnetic fields,<sup>11-22</sup> it is still an important problem not only in the view of theoretical interest but also in the view of experimental interest, and there have been attempts to solve this problem.<sup>23-26</sup> However, unfortunately, some of the relevant works contain inconsistent results on the energy spectral properties: In Ref. 24, Gumbs *et al.* studied the effect of a one-dimensional sine-modulated (1DSM) field on a 2D Bloch electron to argue that the symmetries appeared in the Hofstadter's spectrum break down by the field modulation. Most surprisingly, they also argued that the field modulation leads an additional crisscross pattern like a spiderweb structure onto the Hofstadter's spectrum. However, Oh *et al.*<sup>25</sup> studied the effect of a 1D

cosine-modulated (1DCM) field on a 2D Bloch electron to elucidate that occurrence of gap closing and gap opening leads different energy spectrum from the Hofstadter's spectrum and that the symmetries appeared in the Hofstadter's spectrum except the dual property still remain despite the field modulation. In the meanwhile, Shi and Szeto<sup>26</sup> studied the energy spectrum of a 2D Bloch electron under a kind of 2D field modulation to argue that there is no symmetry breaking in the energy spectrum and that the fractal structure remains irrespective of the field modulation.

In this paper we reexamine the problem of a 2D Bloch electron under spatially modulated magnetic fields to settle the inconsistency discussed above. In doing this, we take into account four kinds of modulated fields (i.e., 1DSM, 1DCM, 2DSM, and 2DCM fields) in order to obtain rather generic effects of the field modulation on the Hofstadter's spectrum. By means of direct diagonalization of the Hamiltonian matrix, we calculate the energy eigenvalues and examine how the system parameters such as the kind of the modulation, the relative strength of the modulated field to the uniform field, and the period of the modulation influence on the energy band structure and the symmetry of the Hofstadter's spectrum. Introduction of the field modulation is shown to change the  $\vec{k}$  dependence of the energy spectrum drastically, leading occurrence of gap opening, gap closing, band crossing, and band broadening, which are the origin of distinctive energy band structure from the Hofstadter's spectrum. Our results indicate that there is no additional spiderweb structure in the energy spectrum contrary to the result of Ref. 24 and that the field modulation generically breaks the symmetries and the fractal property of the Hofstadter's spectrum.

This paper is organized as follows: In Sec. II we introduce four kinds of magnetic fields and the tight-binding model. And, in Sec. III we present numerical results on the energy band structure of a Bloch electron and the symmetries of the energy spectrum under these fields.

Section IV is devoted to a brief summary.

## II. MODULATED MAGNETIC FIELDS AND THE TIGHT-BINDING MODEL

We consider an electron in a 2D square lattice under a spatially modulated magnetic field

$$\vec{B} = [B_0 + B_1(x, y)] \hat{z}, \quad (1)$$

where  $B_0$  ( $B_1$ ) denotes the uniform (modulated) part of an applied magnetic field. Among possible kinds of modulated fields, we pay attention to two kinds of modulated fields. The one is the SM field

$$B_1(x, y) = B_x \sin\left(\frac{2\pi x}{T_x}\right) + B_y \sin\left(\frac{2\pi y}{T_y}\right) \quad (2)$$

and the other is the CM field

$$B_1(x, y) = B_x \cos\left(\frac{2\pi x}{T_x}\right) + B_y \cos\left(\frac{2\pi y}{T_y}\right). \quad (3)$$

Here  $B_{x(y)}$  is the strength of the modulated field and  $T_{x(y)}$  is the period of the modulation along the  $x$  ( $y$ ) direction. Under the Landau gauge, the vector potential becomes

$$\begin{aligned} A_x &= \frac{B_y T_y}{2\pi} \cos\left(\frac{2\pi y}{T_y}\right), \\ A_y &= B_0 x - \frac{B_x T_x}{2\pi} \cos\left(\frac{2\pi x}{T_x}\right) \end{aligned} \quad (4)$$

for the SM field and

$$\begin{aligned} A_x &= -\frac{B_y T_y}{2\pi} \sin\left(\frac{2\pi y}{T_y}\right), \\ A_y &= B_0 x + \frac{B_x T_x}{2\pi} \sin\left(\frac{2\pi x}{T_x}\right) \end{aligned} \quad (5)$$

for the CM field, respectively.

The tight-binding Hamiltonian describing the motion of an electron in a magnetic field is given by

$$H = - \sum_{ij} t_{ij} e^{i\theta_{ij}} |i\rangle \langle j|, \quad (6)$$

where  $t_{ij}$  is the hopping integral between the nearest-neighboring sites  $i$  and  $j$ , and  $\theta_{ij} \equiv (2\pi e/hc) \int_i^j \vec{A} \cdot d\vec{l}$  is the magnetic phase factor. Under the vector potentials given by Eqs. (4) and (5), the magnetic phase factor becomes

$$\theta_{mn; m' n'} = \begin{cases} \pm\theta_m, & (m', n') = (m, n \pm 1) \\ \pm\theta_n, & (m', n') = (m \pm 1, n) \\ 0, & \text{otherwise} \end{cases} \quad (7)$$

with

$$\begin{aligned} \theta_m &= 2\pi m \phi_0 - \beta_x \gamma_x \phi_0 \cos\left(\frac{2\pi m}{\gamma_x}\right), \\ \theta_n &= \beta_y \gamma_y \phi_0 \cos\left(\frac{2\pi n}{\gamma_y}\right) \end{aligned} \quad (8)$$

for the SM field and

$$\begin{aligned} \theta_m &= 2\pi m \phi_0 + \beta_x \gamma_x \phi_0 \sin\left(\frac{2\pi m}{\gamma_x}\right), \\ \theta_n &= -\beta_y \gamma_y \phi_0 \sin\left(\frac{2\pi n}{\gamma_y}\right) \end{aligned} \quad (9)$$

for the CM field, respectively. Here  $\beta_{x(y)} = B_{x(y)}/B_0$ ,  $\gamma_{x(y)} = T_{x(y)}/a$ , and  $\phi_0 = B_0 a^2$ ,  $a$  being the lattice constant. The magnetic flux per unit cell, in units of the flux quantum  $hc/e$ , is given by  $\phi = (1/2\pi) \sum \theta_{ij} = \oint \vec{A} \cdot d\vec{l} = \int \vec{B} \cdot d\vec{S}$ .

By means of Eqs. (6) and (7), the tight-binding equation can be written as

$$\begin{aligned} e^{i\theta_n} \psi_{m+1, n} + e^{-i\theta_n} \psi_{m-1, n} + \lambda (e^{i\theta_m} \psi_{m, n+1} \\ + e^{-i\theta_m} \psi_{m, n-1}) = E \psi_{mn} \end{aligned} \quad (10)$$

where  $\lambda (\equiv t_y/t_x)$  is the ratio of hopping integrals between the  $x$  and  $y$  directions, and  $E$  is the energy in units of  $t_x$ . Here, the wave function is given by  $|\psi\rangle = \sum_j \psi_j |j\rangle$ .

Denoting  $R_{x(y)}$  as the periodicity of  $\theta_{m(n)}$ , the Bloch theorem can be written as

$$\psi_{m+R_x, n} = e^{ik_x R_x} \psi_{mn}, \quad \psi_{m, n+R_y} = e^{ik_y R_y} \psi_{mn}, \quad (11)$$

and the first magnetic Brillouin zone (FMBZ) is given by  $|k_{x(y)}| \leq \pi/R_{x(y)}$ . We calculate the energy eigenvalues for all the values of  $\vec{k}$  in the FMBZ by directly diagonalizing the Hamiltonian matrix obtained from Eqs. (10) and (11).

## III. NUMERICAL RESULTS AND DISCUSSION

In what follows, we assume the modulated field has a square-symmetry (i.e.,  $\beta_x = \beta_y = \beta$  and  $\gamma_x = \gamma_y = \gamma$ ) and consider only the case of the isotropic hopping integral (i.e.,  $\lambda = 1$ ) for the sake of simplicity. And we pay attention to the energy dispersions for  $q = 2, 3$  (with setting  $p = 1$ ) and  $\gamma = 2, 3, 4$  because energy dispersions for other values of  $(q, \gamma)$  can be obtained in a similar way. Here  $p$  and  $q$  denote the numbers (prime each other) given by  $\phi_0 = p/q$ .

## A. Energy spectrum in a uniform magnetic field

In a uniform field ( $\beta = 0$ ),  $\theta_n$  becomes zero. Thus, by means of the translational invariance along the  $y$  direction, Eq. (10) reduces to the Harper equation

$$\psi_{m+1} + \psi_{m-1} + 2 \cos(\theta_m + k_y)\psi_m = E\psi_m, \quad (12)$$

and there are  $q$  eigenvalues for a given value of  $k_y$ . When  $q$  is odd, the full energy spectrum consists of  $q$  subbands. In the meanwhile, when  $q$  is even, the full energy spectrum consists of  $(q - 1)$  subbands because two central subbands touch at zero energy. Here the full energy spectrum means a set of energy eigenvalues obtained by taking into account all the values of  $\vec{k}$  in the FMBZ. Energy dispersions for  $q = 2$  and 3 are given as follows:

(a)  $q = 2$ : We have  $R_x = 2$  and the energy dispersion is given by

$$E(\vec{k}) = \pm 2\sqrt{\cos^2 k_x + \cos^2 k_y}. \quad (13)$$

There are two subbands and they touch at zero energy as shown in Fig. 1(a), resulting a single subband structure with  $|E| \leq 2\sqrt{2}$ .

(b)  $q = 3$ : We have  $R_x = 3$  and the energy dispersion is given by the equation

$$E^3 - 6E - 2(\cos 3k_x + \cos 3k_y) = 0. \quad (14)$$

There are three subbands as shown in Fig. 1(b). But, there is no touching point in the dispersion and the full energy spectrum exhibits a three subband structure with  $-(1 + \sqrt{3}) \leq E \leq -2$ ,  $|E| \leq (\sqrt{3} - 1)$ , and  $2 \leq E \leq (1 + \sqrt{3})$ .

It is well known that the Hofstadter's spectrum has the following symmetries; (i) the dual property between the  $k_x$  and  $k_y$  directions (let us denote it as  $S_D$ ), (ii) the symmetry between  $-E$  and  $E$  ( $S_E$ ), (iii) the symmetry between  $-k_x$  and  $k_x$  ( $S_X$ ), and (iv) the symmetry between  $-k_y$  and  $k_y$  ( $S_Y$ ). It should be noted that  $S_E$  holds only when all the values of  $\vec{k}$  in the FMBZ are taken into account; for a given value of  $\vec{k}$ , one can easily check that  $S_E$  does not hold for odd  $q$ .

## B. Energy spectrum in 1D modulated magnetic fields

When the field modulation is along the  $x$  direction,  $\theta_n$  is still zero and the tight-binding equation is formally the same as Eq. (12). However,  $\beta$  and  $\gamma$  are introduced in  $\theta_m$ , and  $\phi$  becomes periodic along the  $x$  direction with the period  $\gamma$ :

$$\phi/\phi_0 = \begin{cases} 1 + (\beta\gamma/2\pi) [\cos(2\pi(m+1)/\gamma) - \cos(2\pi m/\gamma)] & \text{for 1DSM} \\ 1 - (\beta\gamma/2\pi) [\sin(2\pi(m+1)/\gamma) - \sin(2\pi m/\gamma)] & \text{for 1DCM.} \end{cases} \quad (15)$$

The lattice is called the stripped flux lattice<sup>23</sup> and the energy spectrum can be obtained by diagonalizing the  $(R_x \times R_x)$  Hamiltonian matrix.

### 1. 1DSM Field

When  $(q, \gamma) = (2, 2)$ , we have  $R_x = 2$  and the energy dispersion is given by

$$E(\vec{k}) = 2 \sin \beta \sin k_y \pm 2\sqrt{\cos^2 k_x + \cos^2 \beta \cos^2 k_y}. \quad (16)$$

The two subbands touch at  $(k_x, k_y) = (\pi/2, \pi/2)$  and  $(\pi/2, 3\pi/2)$ , and the energy eigenvalues at the touching points are given by  $E = \pm 2 \sin \beta$ . Since the touching points exist irrespective of  $\beta$ , the full energy spectrum exhibits a single subband structure as in the case of  $\beta = 0$ .

In order to demonstrate the  $\gamma$  dependence of the energy spectrum with  $q = 2$ , we calculate energy spectra for various values of  $\gamma$  and plot some of them in Fig. 2. Even though there are six and four subbands for  $(q, \gamma) = (2, 3)$  and  $(2, 4)$ , there occurs direct touching between the nearest neighboring subbands, which leads a single subband structure of the full energy spectrum. In the calculations, we find that the energy band structure is independent of the values of  $\beta$  and  $\gamma$  while the total bandwidth slightly changes with varying  $\beta$ .

Figure 3 shows the  $k_y$  dependence of the energy spectrum for  $(q, \gamma) = (3, 2)$ . In this case, we have  $R_x = 6$  and there are six subbands. For small values of  $\beta$ , the upper (lower) two subbands touch at several points of  $k_y$ . Besides, there exists indirect overlapping (i.e., crossing of subbands at different values of  $k_y$ ) between the central subbands. Thus, the full energy spectrum still exhibits a three subband structure as can be seen in Fig. 3(a). However, as  $\beta$  increases, there occurs gap opening between the subbands and the full energy spectrum exhibits a six subband structure as in Fig. 3(b). Further increase of  $\beta$  makes the second and the fourth gaps closed, leading a four subband structure as in Fig. 3(c). Figure 4 shows the  $k_y$  dependence of the energy spectrum for  $(q, \gamma) = (3, 3)$ . In this case, we have  $R_x = 3$  and there are three subbands. For small values of  $\beta$ , the full energy spectrum exhibits a three subband structure as in Fig. 4(a). However, indirect overlapping between subbands occurs as  $\beta$  increases, and the full energy spectrum exhibits a single subband structure as in Fig. 4(b). Occurrence of gap closing due to indirect overlapping is also found in the case of  $(q, \gamma) = (3, 4)$ .

As for the symmetry of the energy spectrum, Figs. 2 and 3 show that  $S_E$  remains under the 1DSM field, which is contrary to the arguments of Ref. 24. The reason of this discrepancy lies in the range of  $\vec{k}$  taken into account in discussing the symmetry of the energy spectrum. In Ref. 24 only a particular value of  $\vec{k}$  was taken into account, while all the values of  $\vec{k}$  in the FMBZ are taken

into account in this paper. Here we would like to stress that all the values of  $\vec{k}$  in the FMBZ should be considered in order to discuss the symmetry of the energy spectrum. This is because  $S_E$  of the Hofstadter's spectrum holds only when all the values of  $\vec{k}$  in the FMBZ is considered. We also find that  $S_X$  still remains under the 1DSM field while whether  $S_Y$  remains or not depends crucially on  $q$  and  $\gamma$ . Note that  $S_D$  breaks down by introducing the 1D field modulation.

## 2. 1DCM Field

In order to test how the energy spectrum is influenced on the kind of the field modulation, we also calculate the energy spectrum of a 2D Bloch electron under the 1DCM field. Figure 5 shows the  $k_y$  dependence of the energy spectrum for  $(q, \gamma) = (2, 3)$ . In this case, we have  $R_x = 6$  and there are six subbands. For small values of  $\beta$ , the two central subbands directly touch at two points of  $k_y$  and the upper (lower) two subbands indirectly overlap with each other, resulting a single subband structure as in Fig. 5(a). However, as  $\beta$  increases, indirect overlapping between the upper (lower) two subbands disappears and there occurs gap opening between them. Thus the full energy spectrum exhibits a three subband structure as in Fig. 5(b). Further increase of  $\beta$  makes the remaining indirect overlapping disappear and the full energy spectrum exhibits a five subband structure as in Fig. 5(c). The  $\beta$  dependence of the energy spectrum for  $(q, \gamma) = (2, 4)$  is quite different from  $(q, \gamma) = (2, 3)$ . In this case, we have  $R_x = 4$  and there are four subbands. Each subband directly touches with its neighboring subbands and the full energy spectrum exhibits a single subband structure regardless of  $\beta$ ; the only effect of  $\beta$  is to change the energy bandwidth.

We also perform similar calculations for the energy spectrum with  $q = 3$ . When  $(q, \gamma) = (3, 3)$ , we have  $R_x = 3$  and there are three subbands. For small values of  $\beta$ , the three subbands separate each other, exhibiting a three subband structure as in the case of  $\beta = 0$ . However, as  $\beta$  increases, each subband overlaps indirectly with its neighboring subbands and the gaps between the subbands become closed, resulting a single subband structure. We also find similar phenomena for  $(q, \gamma) = (3, 4)$ .

In Table 1, we summarize the number of subbands of the full energy spectra for the parameters  $(q, \gamma, \beta)$  we took into account. As for the symmetry of the energy spectrum, we find that  $S_E, S_X, S_Y$  remain, while  $S_D$  breaks down under the 1DCM field. Note that  $S_Y$  depends on the kind of the field modulation; it remains (breaks) in the 1DCM (1DSM) field.

Before ending this subsection, we would like to mention two comments. First, we assume  $\gamma$  to be an integer for the sake of simplicity even though it can be arbitrary real value. Besides, we consider only the values of  $\gamma \geq 3$  (2) in the case of the CM (SM) field because  $\phi$  be-

comes nonuniform only under these conditions. However, the authors of Ref. 24 violated this condition; they chose  $\gamma = 1$  in their calculations. But, when  $\gamma = 1$ ,  $\phi$  becomes uniform as can be easily checked by Eq. (15) and the energy spectrum should be identical with the Hofstadter's spectrum if all the values of  $\vec{k}$  in the FMBZ are taken into account, which implies that the results of the cited paper, i.e., the appearance of additional crisscross pattern like a spiderweb structure and the symmetry breaking of the energy spectrum, are erroneous ones coming from mistakes in choosing the values of  $\gamma$  and in choosing the values of  $\vec{k}$ . Note that the method of diagonalization of the Hamiltonian matrix used in the present paper or in the cited paper and the method of the transfer matrix used in Ref. 25 are equivalent. Actually, Fig. 5(a) in the present paper is exactly the same as Fig. 2(b) in Ref. 25. Second, the tight-binding model we are considering is basically a one-band model. Thus, we focus our attention on energy spectra only for the values of  $\beta$  that are not large (i.e.,  $\beta \leq 1$ ) since there might be interband mixing between different Landau levels for large values of  $\beta$ .

## C. Energy spectrum in 2D modulated magnetic fields

When the field modulation is along both lateral directions,  $\theta_n$  becomes nonzero and  $\phi$  becomes periodic in both lateral directions with the period  $\gamma$ . The lattice is called the checkerboard flux lattice<sup>23</sup> and the energy spectrum can be obtained by diagonalizing the  $(R_x R_y \times R_x R_y)$  Hamiltonian matrix.

### 1. 2DSM field

When  $(q, \gamma) = (2, 2)$ , we have  $(R_x, R_y) = (2, 2)$  and the Hamiltonian matrix becomes

$$\begin{pmatrix} 0 & a & b & 0 \\ a^* & 0 & 0 & c \\ b^* & 0 & 0 & d \\ 0 & c^* & d^* & 0 \end{pmatrix} \quad (17)$$

where  $a = -e^{i\beta} - e^{-i(\beta+2k_y)}$ ,  $b = e^{-i\beta} + e^{i(\beta-2k_x)}$ ,  $c = e^{i\beta} + e^{-i(\beta+2k_x)}$ , and  $d = e^{-i\beta} + e^{i(\beta-2k_y)}$ , respectively. By diagonalizing Eq.(17) we obtain the energy dispersion as

$$E(\vec{k}) = \pm 2 \left| \cos \beta \sqrt{\cos^2 k_x + \cos^2 k_y} \pm \sin \beta \sqrt{\sin^2 k_x + \sin^2 k_y} \right|, \quad (18)$$

which is plotted in Fig. 6. Numbering the four subbands in order of lowering energy, one can see that the first (second) and the third (fourth) subbands directly touch

at the center of FMBZ regardless of  $\beta$ . There also exists band crossing between the second and the third subbands, which is absent in the case of the 1D field modulation. Equation (18) indicates that the full energy spectrum exhibits a single subband structure regardless of  $\beta$  and the total bandwidth changes with varying  $\beta$ .

When  $(q, \gamma) = (2, 3)$ , we have  $(R_x, R_y) = (6, 3)$  and there are eighteen subbands. However, due to occurrence of direct touching and indirect overlapping between neighboring subbands, the full energy spectrum exhibits a single subband structure regardless of  $\beta$ . When  $(q, \gamma) = (2, 4)$ , the situation becomes different. In this case, we have  $(R_x, R_y) = (4, 4)$  and there are sixteen subbands. For small values of  $\beta$ , due to direct touching between neighboring subbands, the full energy spectrum exhibits a single subband structure. However, gap opening between subbands occurs with increasing  $\beta$ , resulting a five subband structure of the full energy spectrum.

When  $(q, \gamma) = (3, 2)$ , we have  $(R_x, R_y) = (6, 2)$  and there are twelve subbands. In this case, even for small values of  $\beta$ , the full energy spectrum is quite different from the case of  $\beta = 0$ ; the full energy spectrum exhibits a eight subband structure as can be seen in Fig. 7(a). And, as  $\beta$  increases, two more gaps are open to yield a ten subband structure as in Fig. 7(b). Further increase of  $\beta$  makes the full energy spectrum exhibit a twelve subband structure as in Fig. 7(c). When  $(q, \gamma) = (3, 3)$ , the effect of  $\beta$  is quite different from the case of  $(q, \gamma) = (3, 2)$ . In this case, we have  $(R_x, R_y) = (3, 3)$  and there are nine subbands. For small values of  $\beta$ , the full energy spectrum consists of three subbands as in the case of  $\beta = 0$ . However, there occurs gap closing with increasing  $\beta$  and the energy spectrum exhibits a single subband structure. We also find similar gap closing behavior for  $(q, \gamma) = (3, 4)$ .

## 2. 2DCM Field

In order to know how the energy spectrum is influenced by the kind of the 2D field modulation, we also calculate the energy spectra of a Bloch electron under the 2DCM field with various values of  $(q, \gamma, \beta)$ . And, we find that occurrence of gap closing, gap opening, band crossing, and band broadening is a generic effect of the field modulation.

When  $(q, \gamma) = (2, 3)$ , there are eighteen subbands. For small values of  $\beta$ , due to direct touching and indirect overlapping between the inner sixteen subbands, the full energy spectrum exhibits a three subband structure. However, there occurs gap opening between the inner sixteen subbands with increasing  $\beta$ , resulting a five subband structure. We also find that the widths of gaps broaden with the increase of  $\beta$ . For  $(q, \gamma) = (2, 4)$ , there are sixteen subbands and they compose a single subband structure for small values of  $\beta$ . However, with increasing  $\beta$ , there occurs gap opening and the full energy spectrum exhibits a five subband structure.

When  $(q, \gamma) = (3, 3)$ , there are nine subbands and they compose a three subband structure for small values of  $\beta$ . However, gap closing occurs with increasing  $\beta$ , and the three subband structure becomes a single subband structure. Further increase of  $\beta$  makes the full energy spectrum consist of seven subbands. For  $(q, \gamma) = (3, 4)$ , we show the  $\beta$  dependence of the energy spectrum in Fig. 8, where concurrent occurrence of gap opening and gap closing can be seen. In this case, there are twenty four subbands and they compose a three subband structure for small values of  $\beta$ . However, as  $\beta$  increases, there occurs band splitting and the full energy spectrum exhibits a seven subband structure. Further increase of  $\beta$  makes the full energy spectrum consist of three subbands. We summarize in Table 2 the number of subbands of the full energy spectra for the parameters  $(q, \gamma, \beta)$  taken into account.

The symmetry of the energy spectrum under the 2D modulated fields is rather complicated than the cases of the 1D modulated fields.  $S_E$  remains for both the 2DSM and 2DCM fields as can be seen in Figs. 6–8. However,  $S_X$  and  $S_Y$  depend sensitively on the system parameters. For the parameters considered, we find that  $S_X$  and  $S_Y$  remain for the cases of  $(q, \gamma) = (2, 2), (2, 4), (3, 2)$  in the 2DSM fields and  $(q, \gamma) = (2, 4), (3, 3)$  in the 2DCM fields, while they break for the cases of  $(q, \gamma) = (2, 3), (3, 4)$  in the 2DSM fields and  $(q, \gamma) = (2, 3), (3, 4)$  in the 2DCM fields. In the meanwhile, the energy spectrum in the 2DSM field with  $(q, \gamma) = (3, 3)$  has a flipped symmetry with respect to  $k_{x(y)} = 0$ . Here the flipped symmetry means that the energy spectrum in the range of  $0 \leq k_{x(y)} \leq \pi/R_{x(y)}$  is the same as that in the range of  $-\pi/R_{x(y)} \leq k_{x(y)} \leq 0$  when  $E$  is replaced by  $-E$ .  $S_D$  also depends sensitively on the system parameters; it holds (breaks) for the values of  $(q, \gamma)$  that make  $S_X$  and  $S_Y$  remain (break).

Before ending up this subsection, we would like to mention a few comments. The first is that the above results on  $S_{E(X,Y,D)}$  are not from a theoretical analysis but from a numerical study. Thus, further study such as the group theoretical analysis<sup>23,26,27</sup> is required in order to deepen the understanding of the symmetry breaking. The second is that the  $k_x$  and  $k_y$  directions taken into account in discussing  $S_{X(Y,D)}$  are not the high symmetry directions of the Hamiltonian under the 2D modulated fields. The reason for taking into account these directions, nevertheless, lies in testing how  $S_{X(Y,D)}$  appeared in the Hofstadter's spectrum is influenced by the field modulation. Since symmetry breaking is generally expected if the symmetry axis is not properly chosen, our result that the breaking of  $S_{X(Y,D)}$  depends on the system parameters is quite natural. Finally, it may be worthwhile to note the result of Ref. 26, where Shi and Szeto considered a Bloch electron in the magnetic field

$$\vec{B} = [B_0 + (-1)^{m-n} B_1] \hat{z} \quad (19)$$

and found that there is no symmetry breaking in the energy spectrum and that the fractal structure remains

even though the energy spectrum becomes different from the Hofstadter's spectrum, which seems to be contrary to our results. However, since the directions used in Ref. 26 are the highly symmetric ( $k_x \pm k_y$ ) directions while the directions used in this paper are the  $k_x$  and  $k_y$  directions, it may not be easy to compare both results directly. The only thing we can say is that the field modulation given by in this paper [i.e., Eqs. (1)-(3)] is more generalized than that of Ref. 26 [i.e., Eq. (19)]; specifying the periodic magnetic field by a magnetic unit cell, the lattice with Eq. (19) becomes the simple checkerboard lattice [see, for example, Fig. 2(a) of Ref. 23] while the lattice with Eqs. (1)-(3) becomes a generalized checkerboard lattice [see Fig. 2(b) of Ref. 23]. Thus we expect that the latter may present more generic effect of the field modulation than the former. Further theoretical study on the comparison between two cases is also required.

#### IV. SUMMARY

In summary, we studied the effects of spatially modulated magnetic fields on the Hofstadter's spectrum. In order to obtain rather general properties of the effect of the field modulation, we took into account four kinds of modulated fields and calculated energy eigenvalues with varying  $q$ ,  $\beta$ , and  $\gamma$ . Occurrence of gap opening, gap closing, band crossing, and band broadening was found to be characteristic features of the field modulation, which leads distinctive energy band structure from the Hofstadter's spectrum. It should be noted that these characteristics are very important since the change of the energy dispersion may have crucial influence on the transport properties; it may allow an electron to change its orbit, in view of the semiclassical language. There is also a possibility of quenching the integer quantum Hall behavior and exhibiting normal behavior when the subgaps are smeared out. Sensitive dependence of the energy spectrum on the system parameters implies that it may be difficult to detect direct indication of the Hofstadter's spectrum in experiment since even a tiny change of the magnetic field leads much complicated energy band structure. We also studied the effect of the field modulation on the symmetries appeared in the Hofstadter's spectrum and illustrated that the symmetries sensitively depend on the system parameters. In this work, we have paid attention to the energy spectral properties only with a rational flux and the isotropic hopping integral. Since an introduction of hopping anisotropy is known to lead interesting phenomena like band broadening,<sup>28</sup> it may be interesting to study the effect of hopping anisotropy on the energy spectrum of a 2D Bloch electron under the modulated magnetic fields.

\* Electronic address: ogy@anu.ansung.ac.kr

- <sup>1</sup> R. Peierls, Z. Phys. **80**, 763 (1933); P. G. Harper, Proc. Phys. Soc. London A **68**, 874 (1955); W. Kohn, Phys. Rev. **115**, 1460 (1959); M. Ya Azbel, Sov. Phys. JETP **19**, 634 (1964); D. Langbein, Phys. Rev. **180**, 633 (1969); G. H. Wannier, Phys. Status Solidi B **88**, 757 (1978); G. H. Wannier, G. M. Obermaier, and R. Ray, *ibid.* **93**, 337 (1979); F. H. Claro and G. H. Wannier, Phys. Rev. B **19**, 6068 (1979); A. H. MacDonald, *ibid.* **28**, 6713 (1983); J. B. Sokoloff, Phys. Rep. **126**, 189 (1985); M-C. Chang and Q. Niu, Phys. Rev. B **53**, 7010 (1996); G. Gumbs and P. Fekete, *ibid.* **56**, 3787 (1997).
- <sup>2</sup> D. R. Hofstadter, Phys. Rev. B **14**, 2239 (1976).
- <sup>3</sup> D. J. Thouless, M. Kohmoto, P. Nightingale, and M. Den Nijs, Phys. Rev. Lett. **49**, 405 (1982); R. Rammal, G. Toulouse, M. T. Jaekel, and B. I. Halperin, Phys. Rev. B **27**, 5142 (1983); M. Kohmoto, *ibid.* **39**, 11943 (1989); Y. Hatsugai and M. Kohmoto, *ibid.* **42**, 8282 (1990).
- <sup>4</sup> P. W. Anderson, Phys. Scr. T **27**, 60 (1989); P. Lederer, D. Poilblanc, and T. M. Rice, Phys. Rev. Lett. **63**, 1519 (1989).
- <sup>5</sup> S. Alexander, Phys. Rev. B **27**, 1541 (1983); R. Rammal, T. C. Lubensky and G. Toulouse, *ibid.* **27**, 2820 (1983); Q. Niu and F. Nori, *ibid.* **39**, 2134 (1989).
- <sup>6</sup> B. Pannetier, J. Chaussy, R. Rammal, and J-C. Villegier, Phys. Rev. Lett. **53**, 1845 (1984).
- <sup>7</sup> D. Weiss, M. L. Roukes, A. Menshig, P. Grambow, K. von Klitzing, and G. Wieman, Phys. Rev. Lett. **66**, 2790 (1991).
- <sup>8</sup> A. Lorke, J. P. Kotthaus, and K. Ploog, Phys. Rev. B **44**, 3447 (1991).
- <sup>9</sup> R. R. Gerhardts, D. Weiss, and U. Wulf, Phys. Rev. B **43**, 5192 (1991); R. R. Gerhardts and D. Pfannkuche, Surf. Sci. **263**, 324 (1992).
- <sup>10</sup> P. A. Lee and D. S. Fisher, Phys. Rev. Lett. **47**, 882 (1981); H. Aoki and T. Ando, *ibid.* **54**, 831 (1985); B. Huckestein and B. Kramer, *ibid.* **64**, 1437 (1990); Y. Avishi and R. M. Redheffer, Phys. Rev. B **47**, 2089 (1993).
- <sup>11</sup> D. Yoshioka and Y. Iye, J. Phys. Soc. Jpn. **56**, 448 (1987).
- <sup>12</sup> D. P. Xue and G. Xiao, Phys. Rev. B **45**, 5986 (1992).
- <sup>13</sup> F. M. Peeters and P. Vasilopoulos, Phys. Rev. B **47**, 1466 (1993).
- <sup>14</sup> X. Wu and S. E. Ulloa, Phys. Rev. B **47**, 10028 (1993).
- <sup>15</sup> G. J. O. Schmidt, Phys. Rev. B **47**, 13007 (1993).
- <sup>16</sup> R. B. S. Oakeshott and A. MacKinnon, J. Phys. Condens. Matter **5**, 9355 (1993).
- <sup>17</sup> R. Yagi and Y. Iye, J. Phys. Soc. Jpn. **62**, 1279 (1993).
- <sup>18</sup> P. Schmelcher and D. L. Shepelyansky, Phys. Rev. B **49**, 7418 (1994).
- <sup>19</sup> S. M. Stewart and C. Zhong, J. Phys. Condens. Matter **8**, 6019 (1996).
- <sup>20</sup> S. Izawa, S. Katsamoto, A. Endo, and Y. Iye, J. Phys. Soc. Jpn. **64**, 706 (1995).
- <sup>21</sup> H. A. Carmona, A. K. Geim, A. Nogaret, P. C. Main, T. I. Foster, M. Henini, S. P. Beaumont, and M. G. Blamire, Phys. Rev. Lett. **74**, 3009 (1995).
- <sup>22</sup> P. D. Ye, D. Weiss, R. R. Gerhardts, M. Seeger, K. von Klitzing, K. Eberl, and H. Nickel, Phys. Rev. Lett. **74**, 3013 (1995).

- <sup>23</sup> A. Barelli, J. Bellissard, and R. Rammal, J. Phys. (Paris) **51**, 2167 (1990).
- <sup>24</sup> G. Gumbs, D. Miesse, and D. Huang, Phys. Rev. B **52**, 14755 (1995).
- <sup>25</sup> G. Y. Oh, J. Jang, and M. H. Lee, J. Korean Phys. Soc. **29**, 79 (1996); G. Y. Oh and M. H. Lee, Phys. Rev. B **53**, 1225 (1996).
- <sup>26</sup> Q. W. Shi and K. Y. Szeto, Phys. Rev. B **56**, 9251 (1997).
- <sup>27</sup> M. C. Chang and Q. Niu, Phys. Rev. B **50**, 10843 (1994); Y. Hatsugai, M. Kohmoto, and Y-S. Wu, *ibid.* **53**, 9697 (1996); M. C. Chang and M. F. Yang, *ibid.* **57**, 13002 (1998).
- <sup>28</sup> S. N. Sun and J. P. Ralston, Phys. Rev. B **44**, 13603 (1991); G. Y. Oh, J. Jang, and M. H. Lee, J. Korean Phys. Soc. **29**, 261 (1996).

## FIGURE CAPTIONS

**Fig. 1** Energy dispersion in the uniform magnetic field with (a)  $q = 2$  and (b)  $q = 3$ . The horizontal plane is drawn in units of  $\pi$ .

**Fig. 2** Plot of  $E$  versus  $k_y$  in the 1DSM field with  $\beta = 0.3$ , where (a)  $(q, \gamma) = (2, 3)$  and (b)  $(q, \gamma) = (2, 4)$ . The horizontal axis is drawn in units of  $\pi$ .

**Fig. 3** Plot of  $E$  versus  $k_y$  in the 1DSM field with  $(q, \gamma) = (3, 2)$ , where (a)  $\beta = 0.3$ , (b)  $\beta = 0.6$ , and (c)  $\beta = 0.9$ .

**Fig. 4** Plot of  $E$  versus  $k_y$  in the 1DSM field with  $(q, \gamma) = (3, 3)$ , where (a)  $\beta = 0.3$  and (b)  $\beta = 0.9$ .

**Fig. 5** Plot of  $E$  versus  $k_y$  in the 1DCM field with  $(q, \gamma) = (2, 3)$ , where (a)  $\beta = 0.3$ , (b)  $\beta = 0.6$ , and (c)  $\beta = 0.9$ .

**Fig. 6** Energy dispersion in the 2DSM field with  $(q, \gamma) = (2, 2)$ , where (a)  $\beta = 0.3$  and (b)  $\beta = 0.9$ .

**Fig. 7** Plot of  $E$  versus  $k_y$  in the 2DSM field with  $(q, \gamma) = (3, 2)$ , where (a)  $\beta = 0.3$ , (b)  $\beta = 0.6$ , and (c)  $\beta = 0.9$ .

**Fig. 8** Plot of  $E$  versus  $k_y$  in the 2DCM field with  $(q, \gamma) = (3, 4)$ , where (a)  $\beta = 0.3$  and (b)  $\beta = 0.6$ .

## TABLE CAPTIONS

**Table 1** Number of subbands of the full energy spectrum under the 1D modulated fields.

**Table 2** Number of subbands of the full energy spectrum under the 2D modulated fields.

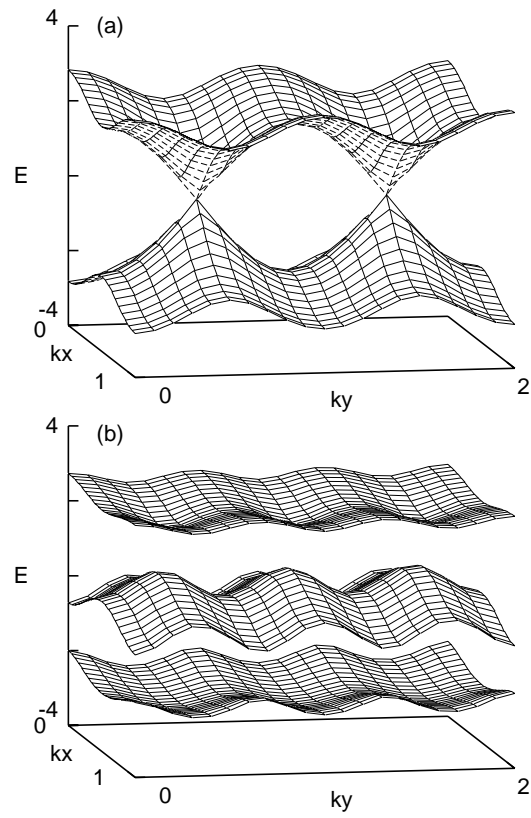


Fig.1 : Gi-Yeong Oh

kind		1DSM						1DCM			
$q$		2			3			2		3	
$\gamma$		2	3	4	2	3	4	3	4	3	4
$\beta$	0.3	1	1	1	3	3	3	1	1	3	3
	0.6	1	1	1	6	1	1	3	1	1	1
	0.9	1	1	1	4	1	1	5	1	1	1

**Table 1 : Gi-Yeong Oh**

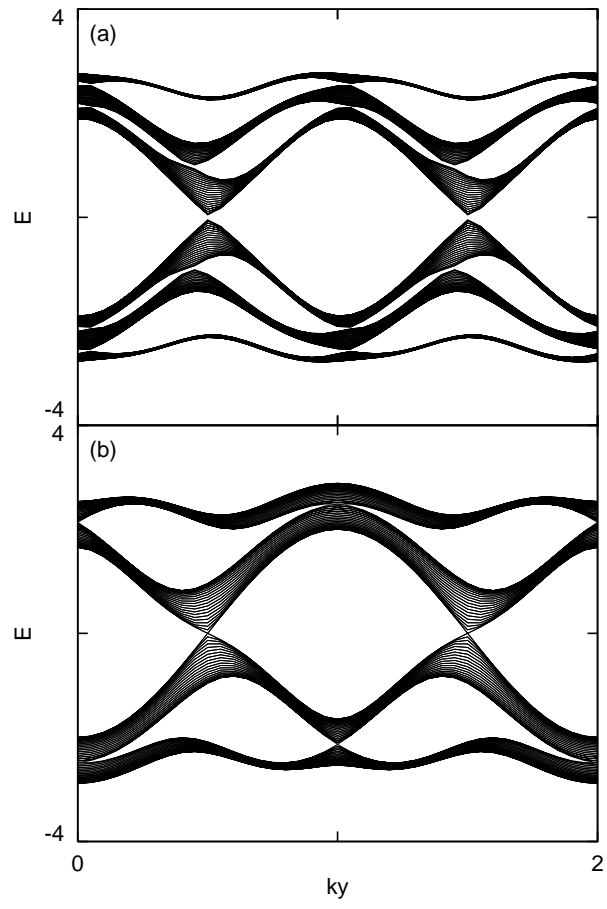


Fig.2 : Gi-Yeong Oh

kind		2DSM						2DCM			
$q$		2			3			2		3	
$\gamma$		2	3	4	2	3	4	3	4	3	4
$\beta$	0.3	1	1	1	8	3	7	3	1	3	3
	0.6	1	1	5	10	3	7	5	5	1	7
	0.9	1	1	5	12	3	5	5	5	7	3

**Table 2 : Gi-Yeong Oh**

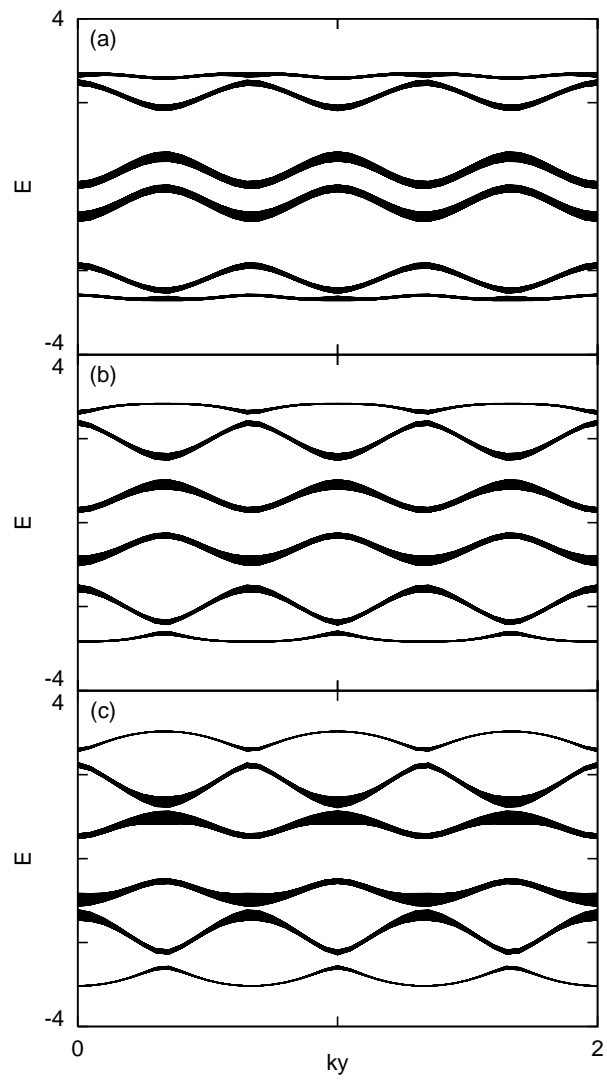


Fig.3 : Gi-Yeong Oh

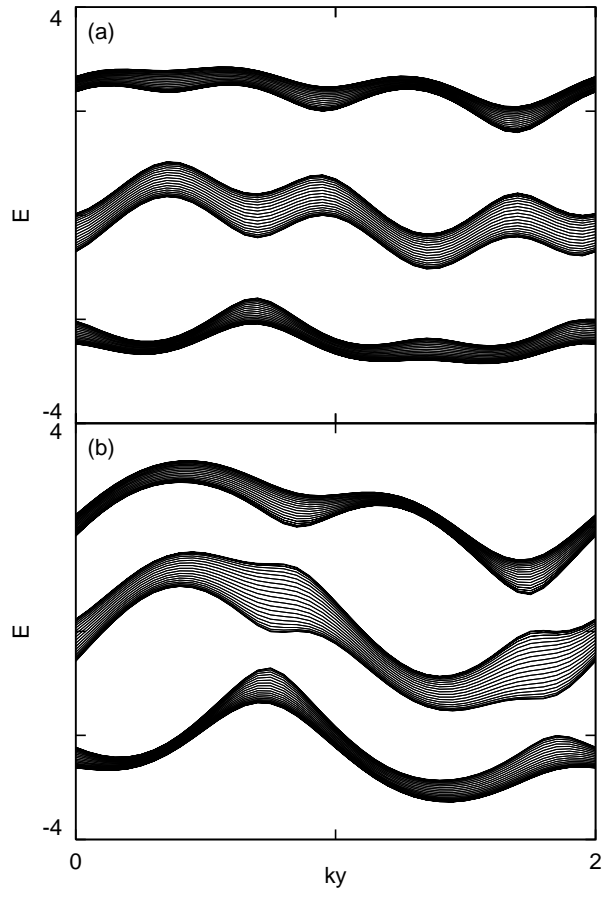


Fig.4 : Gi-Yeong Oh

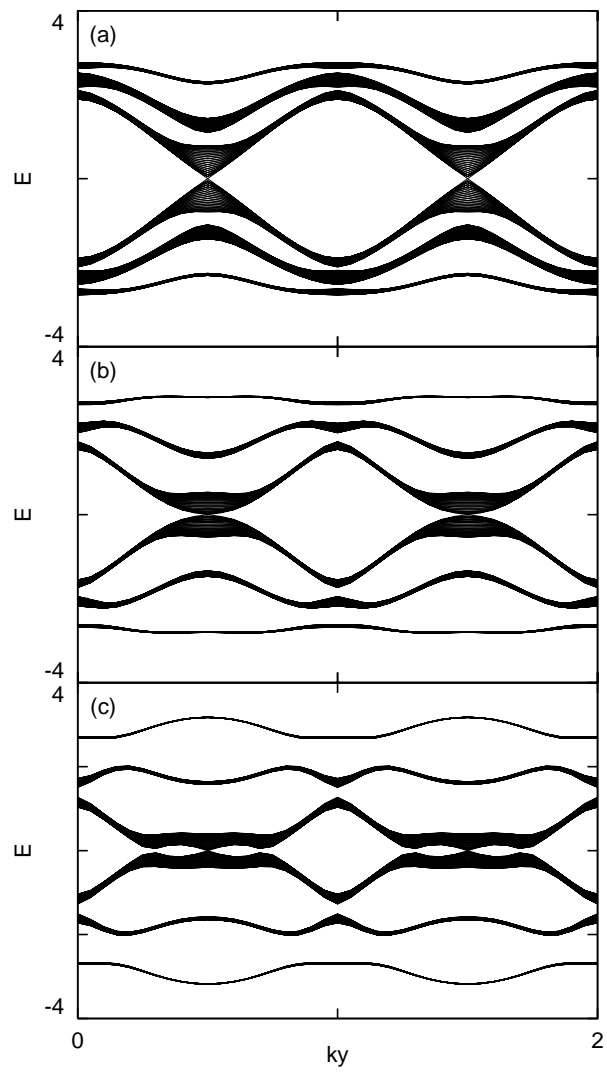


Fig.5 : Gi-Yeong Oh

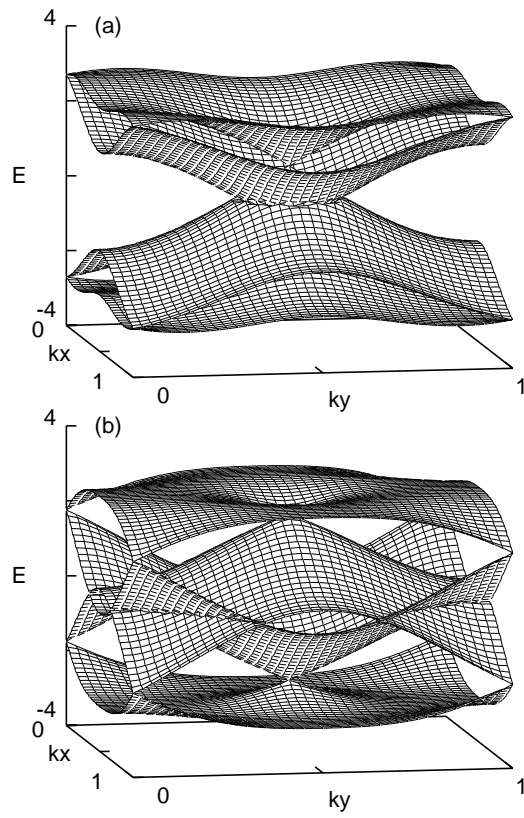


Fig.6 : Gi-Yeong Oh

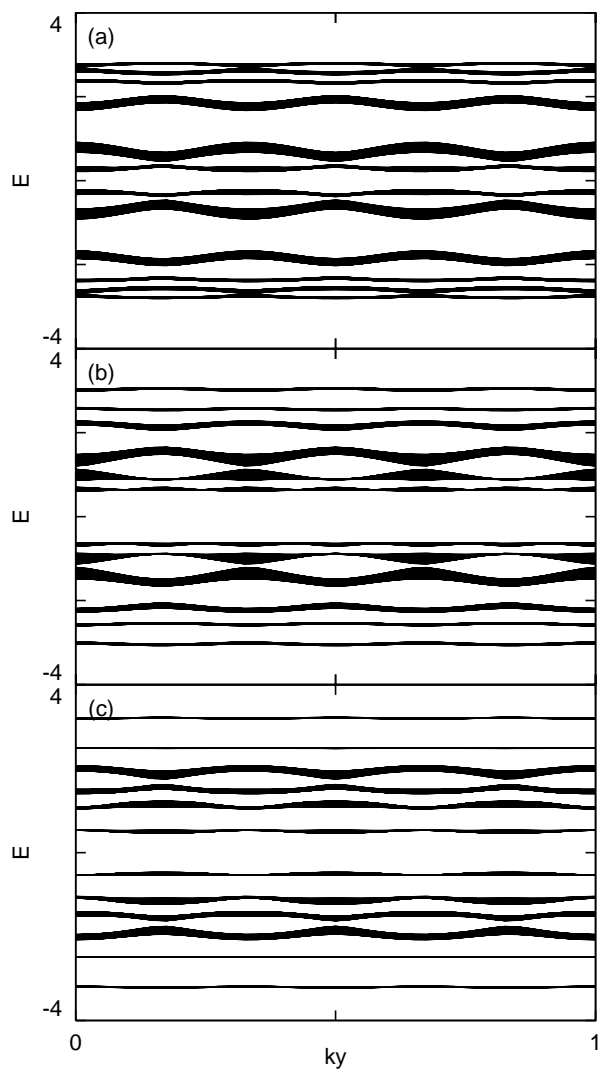


Fig.7 : Gi-Yeong Oh

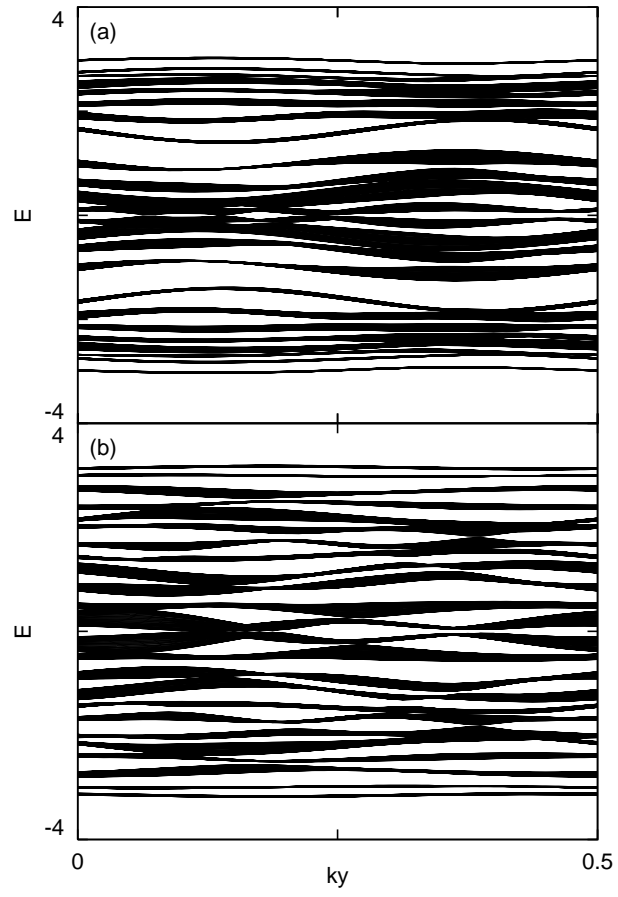


Fig.8 : Gi-Yeong Oh